Supporting Information

New Two-Dimensional Ge-Sb-Te Semiconductors with High Photovoltaic Performance for Solar Energy Conversion

Yu Gan,[1] Naihua Miao,[1,2] Jian Zhou[1] and Zhimei Sun[1,2,*]

[1]School of Materials Science and Engineering, Beihang University, Beijing 100191, China

[2]Center for Integrated Computational Materials Engineering, International Research Institute for Multidisciplinary Science, Beihang University, Beijing 100191, China

*Corresponding authors: zmsun@buaa.edu.cn (Z. M. Sun)

■ Calculation of the optical absorption coefficient

Using the frequency-dependent dielectric functions ($\varepsilon(\omega)=\varepsilon_1(\omega)+i\varepsilon_2(\omega)$), the optical absorption coefficient $\alpha(\omega)$ is estimated based on the following equation:[1]

$$\alpha(\omega)=\sqrt{2}\omega\left(\sqrt{\varepsilon_1^2(\omega)+\varepsilon_2^2(\omega)}-\varepsilon_1(\omega)\right)^{1/2}. \quad (1)$$

$\varepsilon_1(\omega)$ is the real part of dielectric functions, which is defined by the usual Kramers-Kronig transformation:[1,2]

$$\varepsilon_1(\omega)=1+\frac{2}{\pi}P\int_0^\infty \frac{\varepsilon_2(\omega')\omega'}{\omega'^2-\omega^2+i\eta}d\omega', \quad (2)$$

where P is the Cauchy principal values. $\varepsilon_2(\omega)$ is imaginary part of dielectric functions and can be determined by the summation over empty states:

$$\varepsilon_2(\omega)=\frac{4\pi^2e^2}{\Omega}\lim_{q\to 0}\frac{1}{q^2}\sum_{c,v,\mathbf{k}}2\omega_{\mathbf{k}}\delta\left(\varepsilon_{c\mathbf{k}}-\varepsilon_{v\mathbf{k}}-\omega\right)\times\left\langle u_{c\mathbf{k}}+e_{\alpha\mathbf{k}}\left|u_{v\mathbf{k}}\right\rangle\right\langle u_{c\mathbf{k}}+e_{\beta\mathbf{k}}\left|u_{v\mathbf{k}}\right\rangle\right.^{*}, \tag{3}$$

where v and c indicate the valence- and conduction-band states, respectively, and $u_{c\mathbf{k}}$ is the lattice cell periodic part of the electron orbitals at k-point, $\mathbf{k}$.

■ Estimation of the photovoltaic conversion efficiency

The photovoltaic (PV) efficiency is defined as:

$$\xi = P_m / P_{in} \times 100\%, \tag{4}$$

where P_m is the maximum output power density and P_{in} indicates the total incident solar-energy density from the solar spectrum. P_m is determined by maximizing the product of voltage V and current density J using the formula:[3,4]

$$P_m = JV = \left(J_{sc} - J_0\left(e^{eV/k_BT} - 1\right)\right)V. \tag{5}$$

Within this equation, J_{sc} and J_0 are the short-circuit and reverse-saturation current densities, respectively, which can be calculated by:

$$J_{sc} = e\int_0^{\infty} a(E)I_s(E)dE, \tag{6}$$

$$J_0 = \frac{e\pi}{f_r}\int_0^{\infty} a(E)I_b(E,T)dE. \tag{7}$$

$a(E)$ is the photon absorptivity, closely related to the light absorption:

$$a(E) = 1 - e^{-2\alpha(\omega)L}, \tag{8}$$

where L, $I_s(E)$ and $I_b(E,T)$ are the thickness of PV absorber, the AM1.5G solar spectrum and the black-body spectrum, respectively. f_r represents the fraction of the radiative electron-hole recombination current:

$$f_r = e^{-\Delta E_g / k_B T} = e^{-\left(E_g^{da} - E_g\right)/k_B T}. \quad (9)$$

E_g^{da} and E_g are the direct-allowed and fundamental bandgaps, respectively. Thus for a direct bandgap semiconductor, f_r =1.

■ Computation of the formation energy

The formation energy (E_f , in the units of eV/atom) of $Ge_xSb_yTe_z$ compounds is calculated from

$$E_f = \left(E_{Ge_xSb_yTe_z} - xE_{Ge} - yE_{Sb} - zE_{Te}\right) / \left(x + y + z\right), \quad (10)$$

where $E_{Ge_xSb_yTe_z}$ is the total energy of GST monolayers; E_{Ge} , E_{Sb} , and E_{Te} are the total energy of Ge, Sb and Te bulk crystals, respectively.

■ Calculation of the carrier effective mass

The electron and hole effective masses (m_e^* and m_h^*) of GST monolayers were calculated from the second derivatives of energy of the lowest conduction band (LCB) and the highest valence band (HVB) near the conduction band minimum (CBM) and the valence band maximum (VBM), respectively. Specifically, m_e^* and m_h^* were calculated according to the equations: $\frac{1}{m_e^*} = \frac{1}{\hbar^2}\frac{\partial^2 E_c}{\partial^2 k}$, $\frac{1}{m_h^*} = \frac{1}{\hbar^2}\frac{\partial^2 E_v}{\partial^2 k}$, where E_c and E_v are the energy near the CBM and VBM, respectively, and k represents the wave vector. It is clearly seen from Fig. S4 that the electronic bands near the CBM and VBM of the three GST

monolayers are very dispersive, thereby leading to a very small hole and electron effective masses, as shown in Table S1. Notably, there are two directions around the VBM (m_{h1}^* and m_{h2}^*) and CBM (m_{e1}^* and m_{e2}^*), and here $m_h^*=\sqrt{m_{h1}^* \cdot m_{h2}^*}$ ($m_e^*=\sqrt{m_{e1}^* \cdot m_{e2}^*}$) was adopted to describe the hole (electron) effective mass.

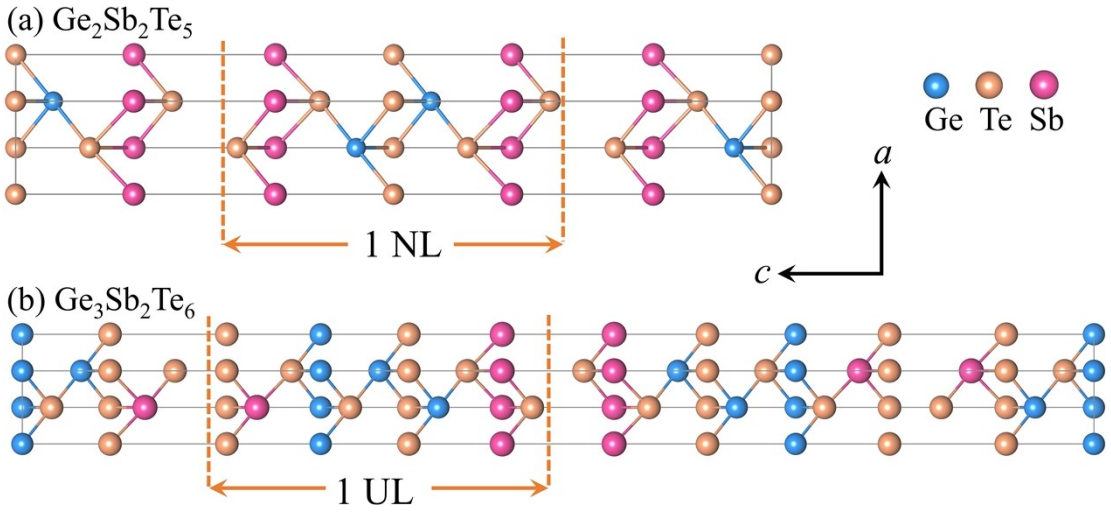

Fig. S1 Crystal structures of (a) $Ge_2Sb_2Te_5$ and (b) $Ge_3Sb_2Te_6$.

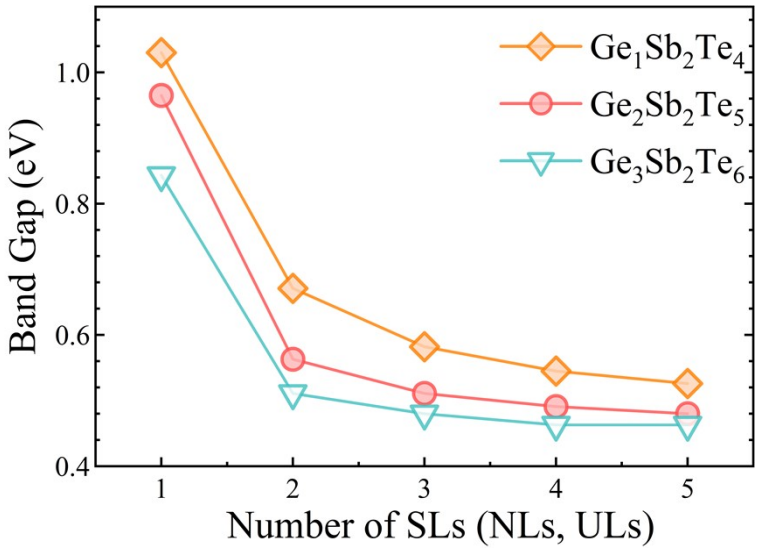

Fig. S2 Calculated electronic bandgaps of 2D GST compounds with different number of SLs (NLs, ULs), using the HSE06 functional.

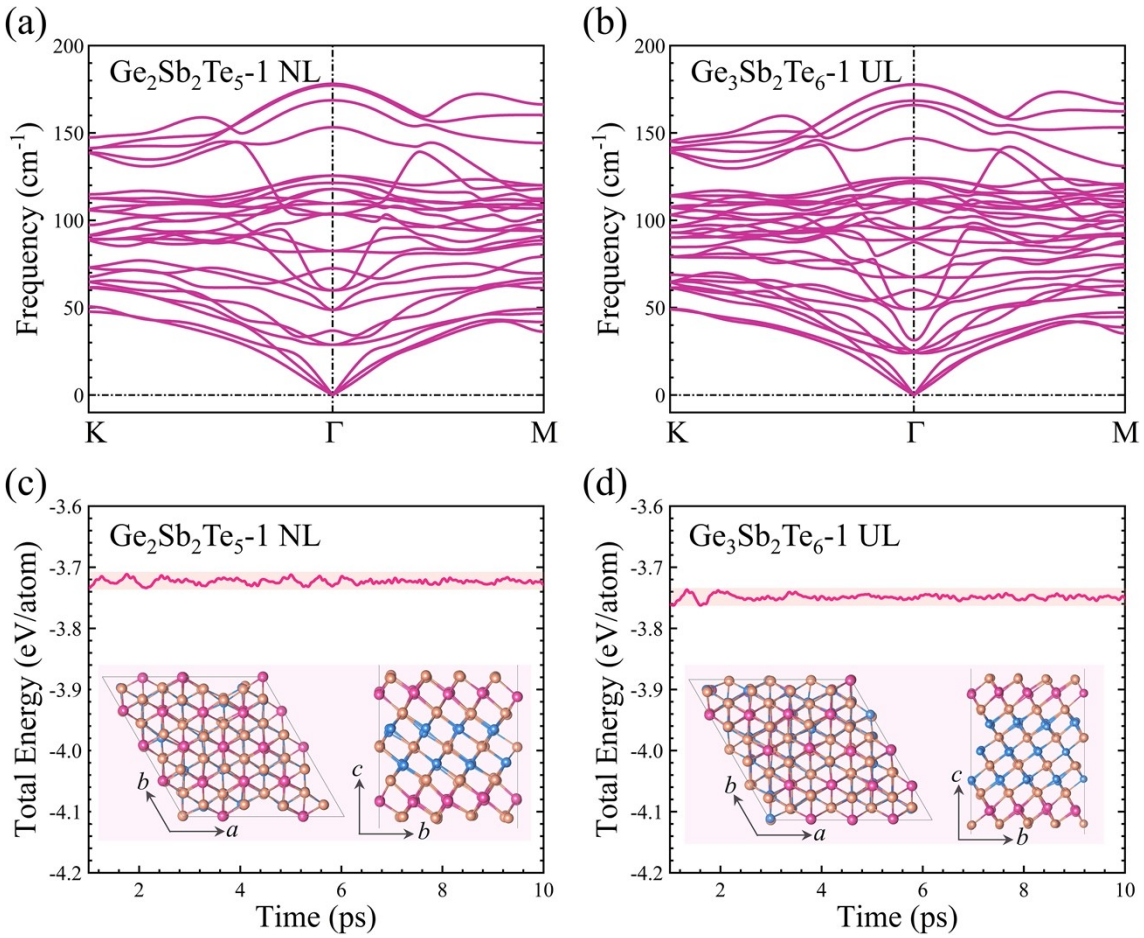

Fig. S3 (a, b) Phonon dispersion curves and (c, d) total energy evolution in AIMD simulations at 300 K for (a, c) $Ge_2Sb_2Te_5$-1 NL and (b, d) $Ge_3Sb_2Te_6$-1 UL. The insets in (c, d) are the crystal structures at 10 ps.

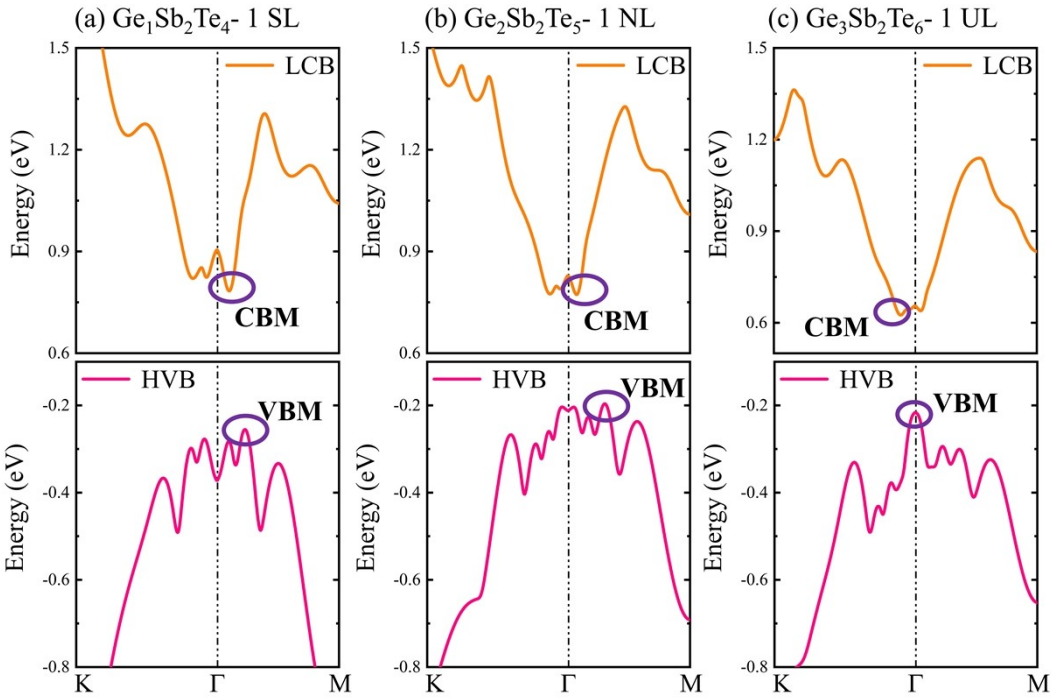

Fig. S4 The highest valence band (HVB) and lowest conduction band (LCB) of (a) $Ge_1Sb_2Te_4$-1 SL, (b) $Ge_2Sb_2Te_5$-1 NL and (c) $Ge_3Sb_2Te_6$-1 UL.

Table S1 Hole and electron effective masses (m_e^* and m_h^*) for GST monolayers. Subscripts 1 and 2 represent the effective mass in two different directions (i.e., 1: left, 2: right), respectively.

Compound	m_{h1}^*	m_{h2}^*	m_{e1}^*	m_{e2}^*	m_h^*	m_e^*
$Ge_1Sb_2Te_4$-1 SL	0.12	0.14	0.16	0.08	0.13	0.12
$Ge_2Sb_2Te_5$-1 NL	0.16	0.17	0.22	0.08	0.17	0.14
$Ge_3Sb_2Te_6$-1 UL	0.21	0.21	0.21	0.33	0.21	0.26

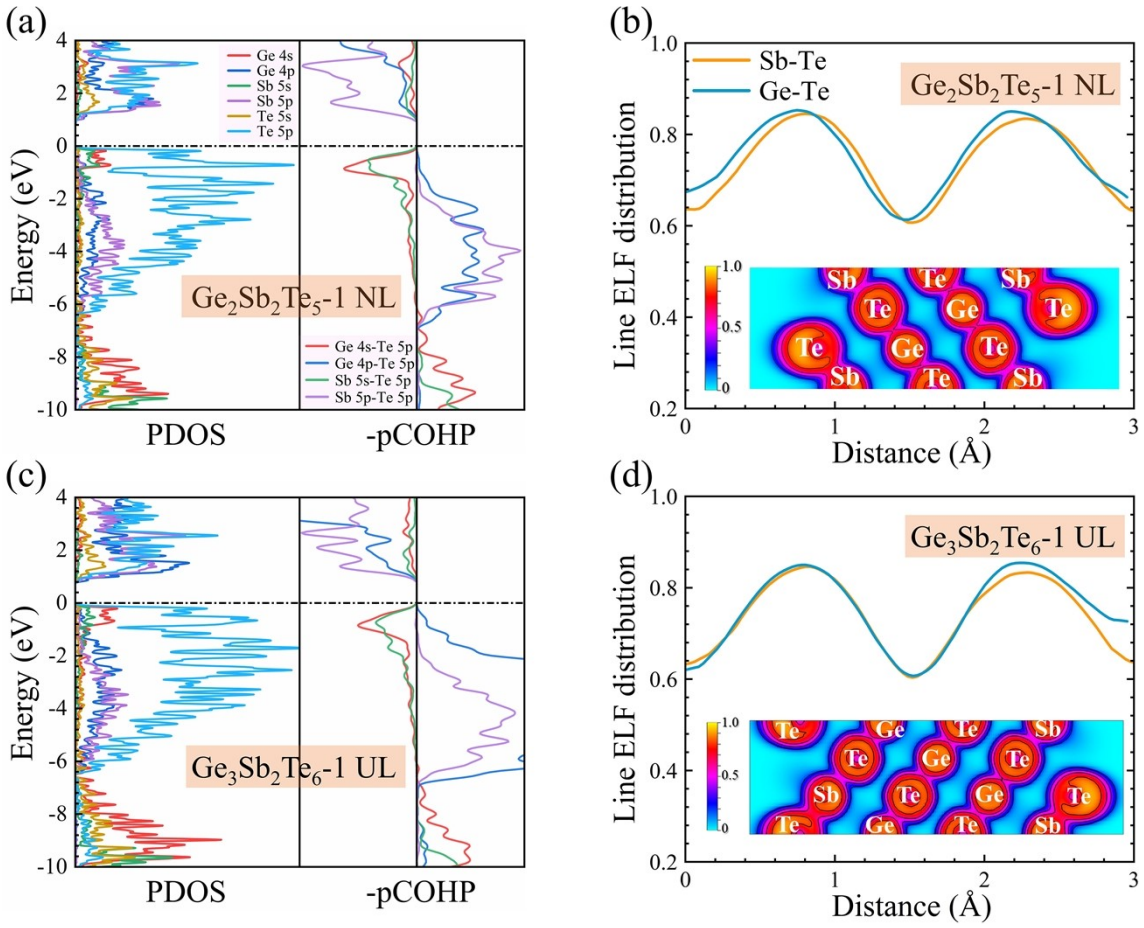

Fig. S5 (a, c) Projected density of states (left panel), pCOHP (right panel) and (b, d) ELF of (a, b) $Ge_2Sb_2Te_5$-1 NL and (c, d) $Ge_3Sb_2Te_6$-1 UL. The Fermi energy is set to 0 eV.

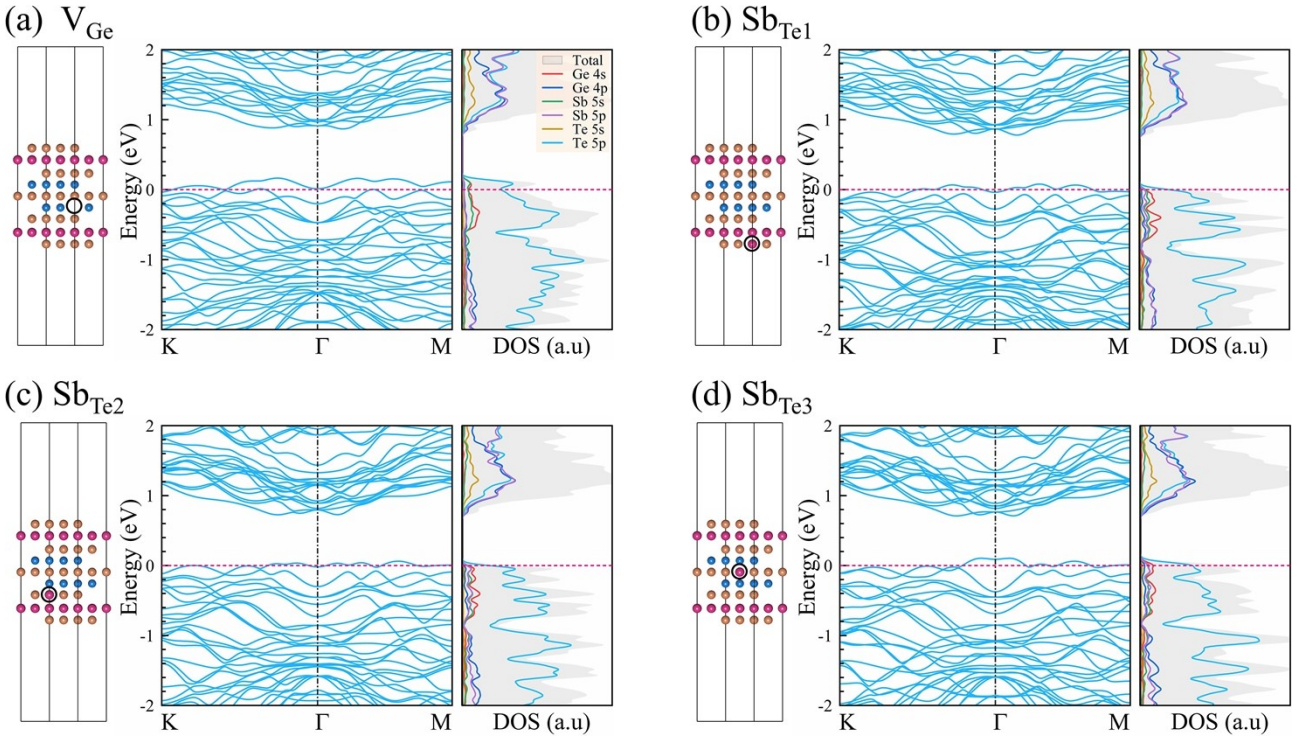

Fig. S6 The 2×2×1 supercells of defective $Ge_2Sb_2Te_5$-1 NL containing (a) a Ge vacancy, (b) a Sb_{Te1} antisite, (c) a Sb_{Te2} antisite, and (d) a Sb_{Te3} antisite as well as the corresponding electronic band structures and density of states. The Fermi energy is set to 0 eV (red dashed lines).

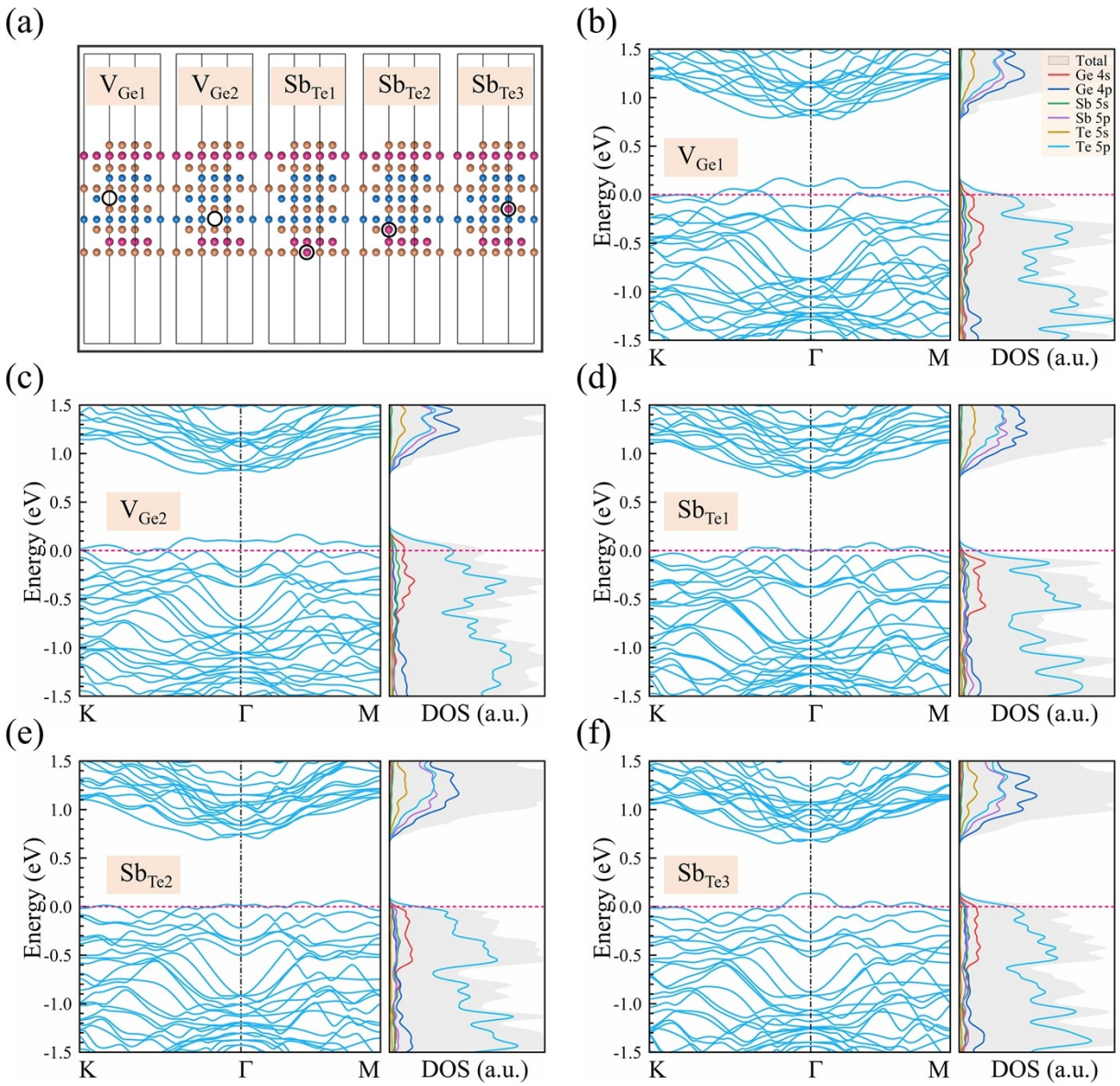

Fig. S7 (a) The 2×2×1 supercells of defective $Ge_3Sb_2Te_6$-1 UL and (b-f) corresponding electronic structures. The Fermi energy is set to 0 eV (red dashed lines).

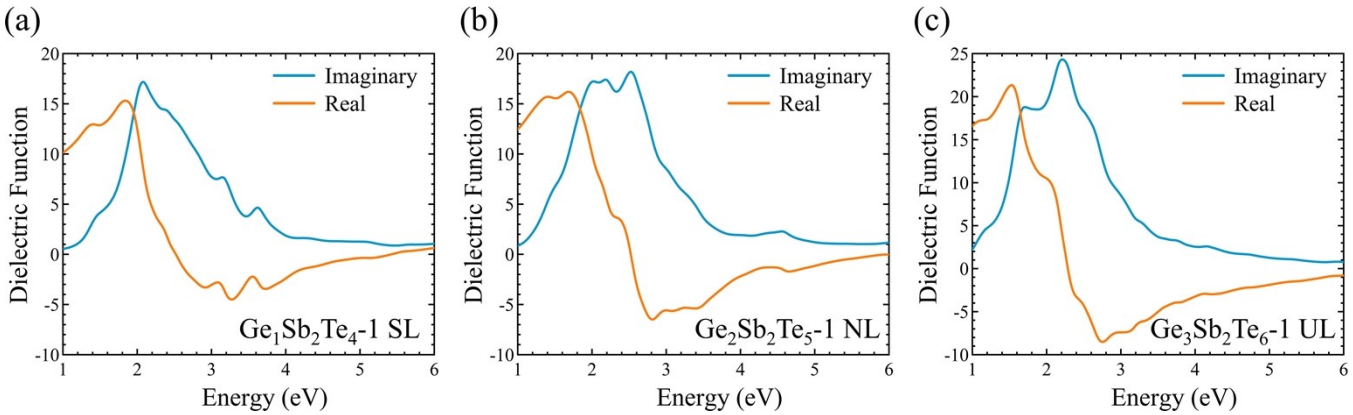

Fig. S8 Calculated dielectric functions of (a) $Ge_1Sb_2Te_4$-1 SL, (b) $Ge_2Sb_2Te_5$-1 NL and (c) $Ge_3Sb_2Te_6$-1 UL using the HSE06 method.

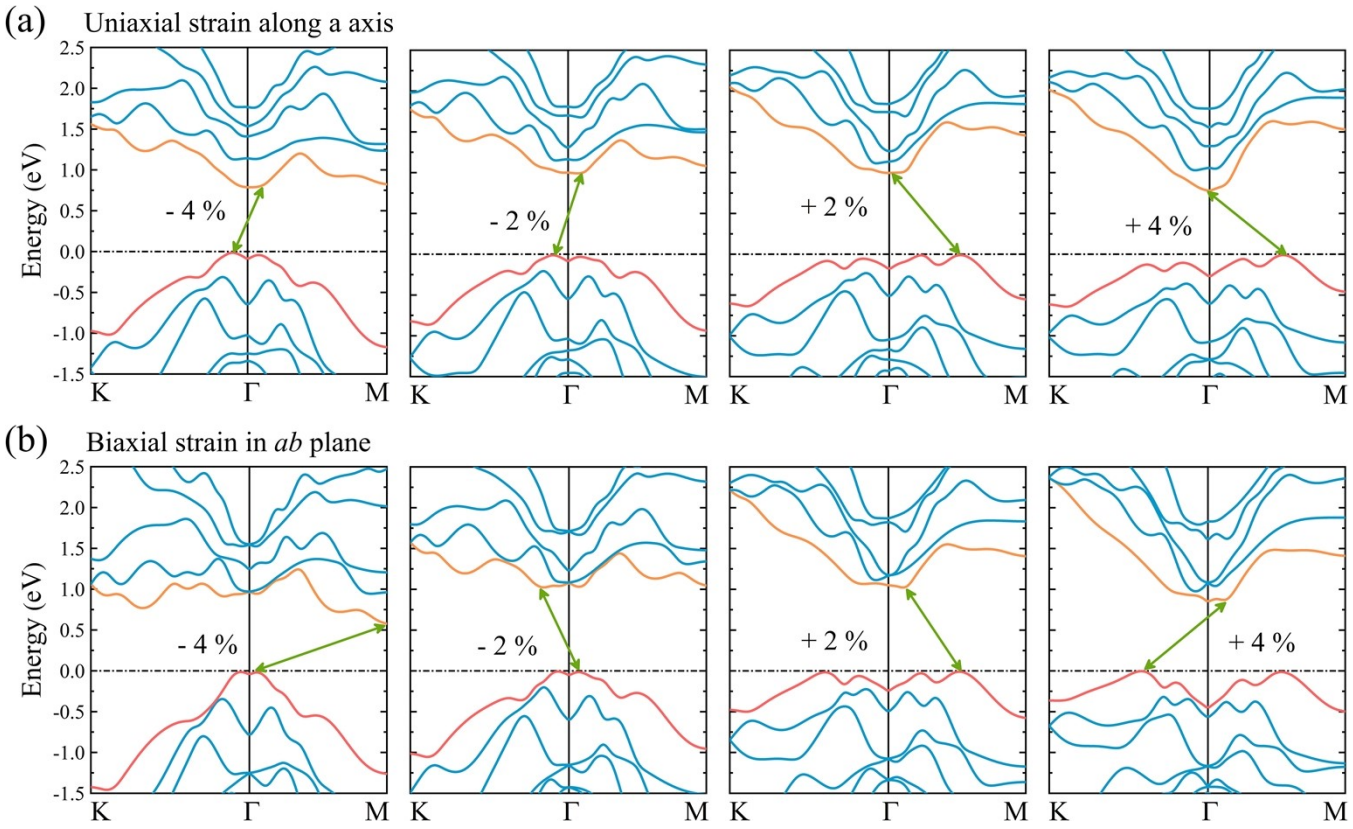

Fig. S9 Calculated band structures of $Ge_1Sb_2Te_4$-1 SL under different (a) uniaxial and (b) biaxial strains.

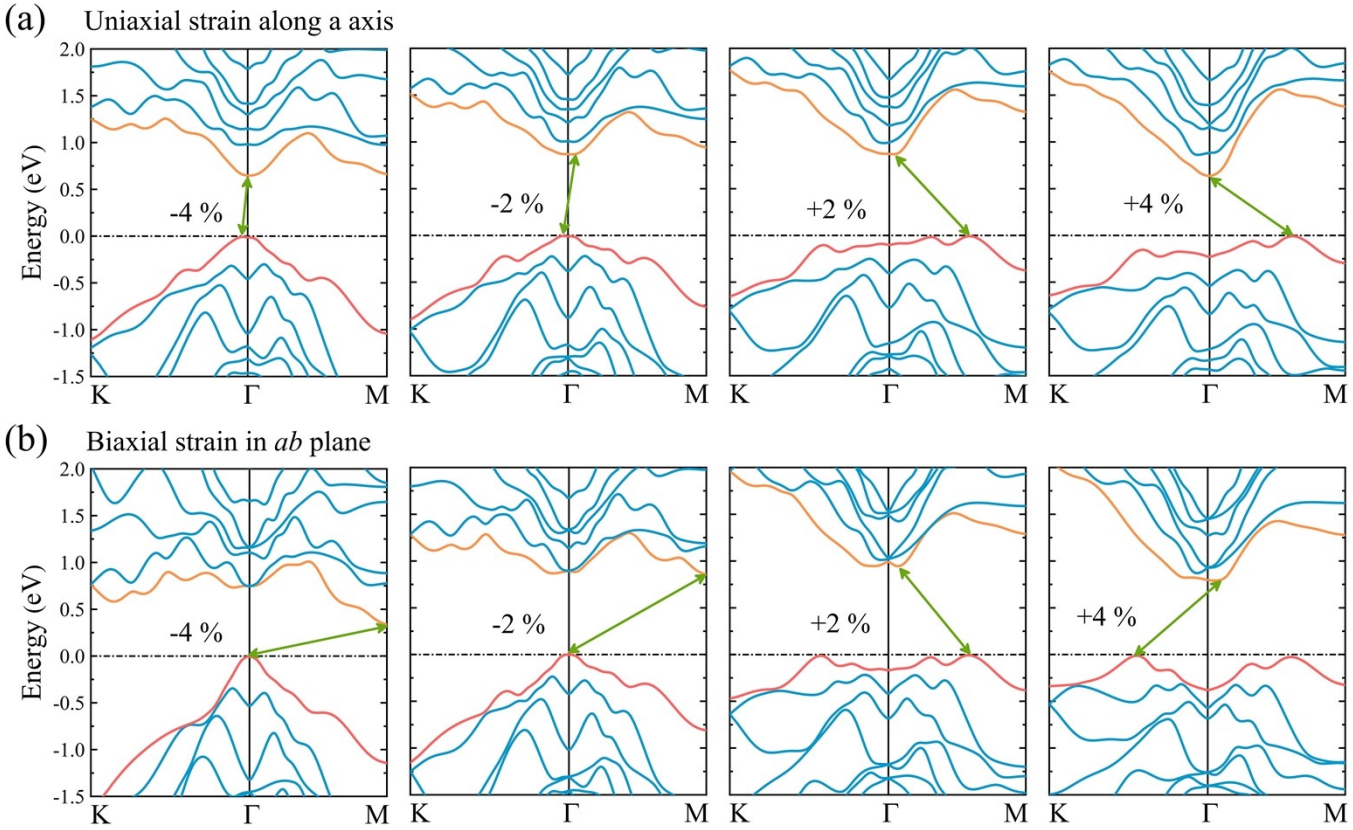

Fig. S10 Electronic band structures of $Ge_2Sb_2Te_5$-1 NL under different (a) uniaxial and (b) biaxial strains.

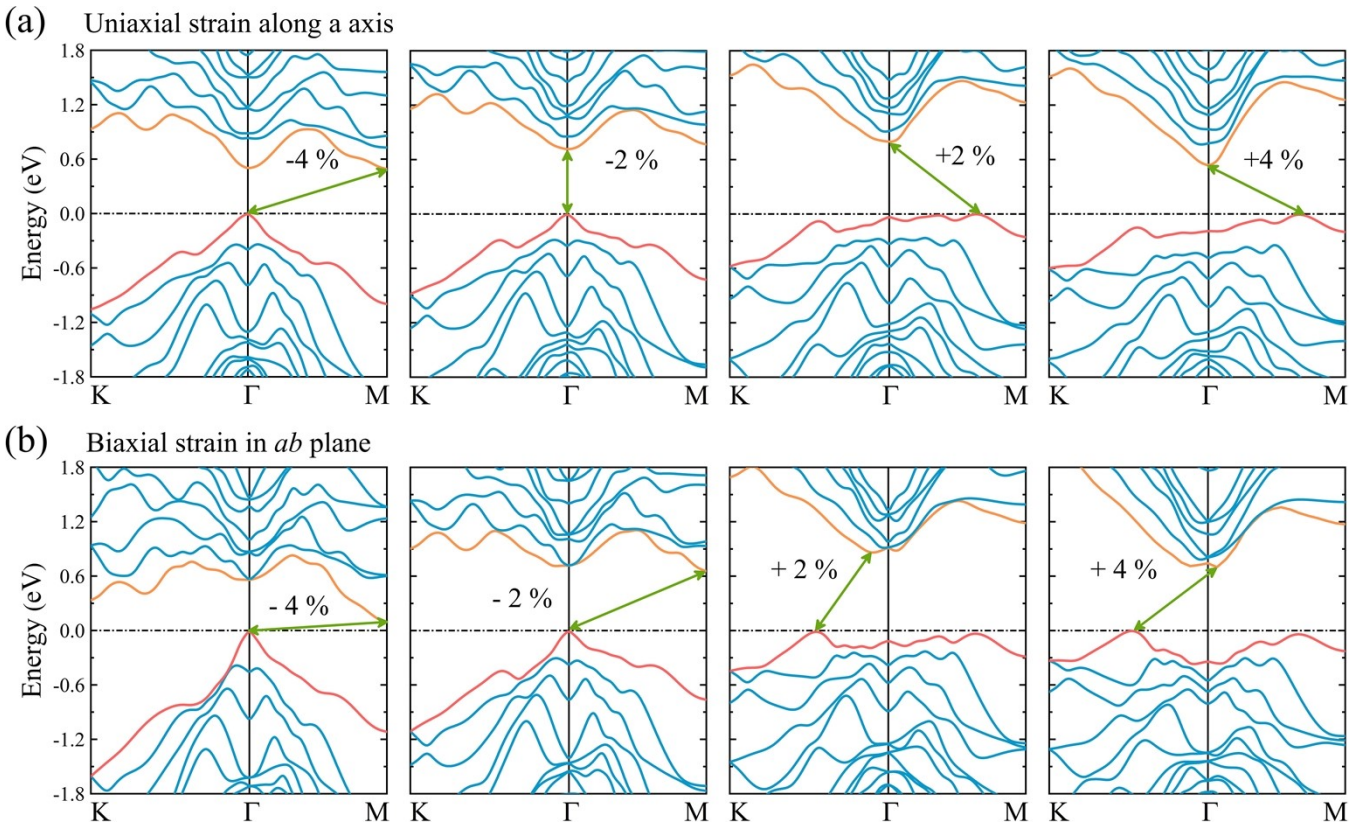

Fig. S11 Electronic band structures of $Ge_3Sb_2Te_6$-1 UL under different (a) uniaxial and (b) biaxial strains.

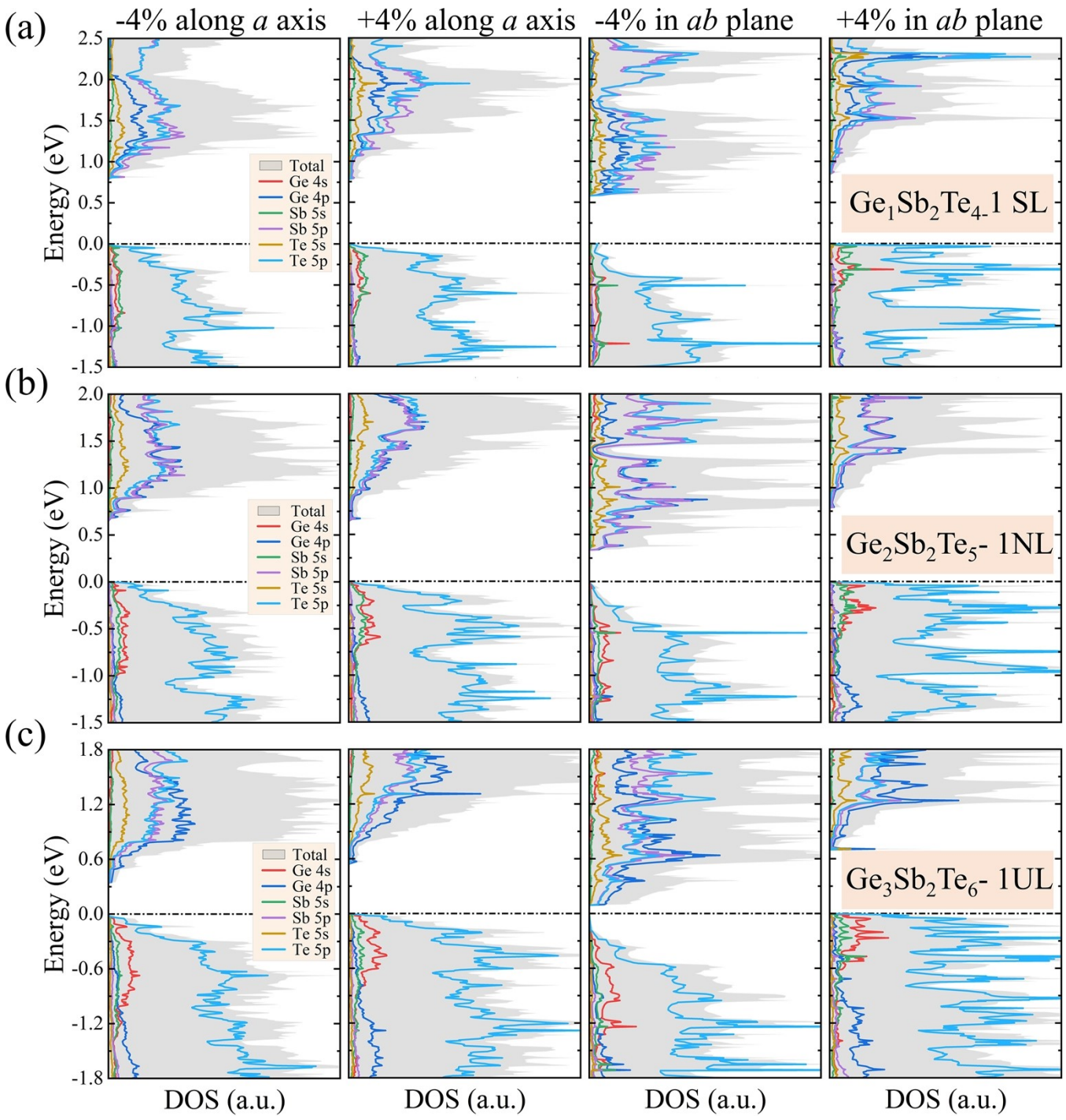

Fig. S12 Calculated density of states of (a) $Ge_1Sb_2Te_4$-1 SL, (b) $Ge_2Sb_2Te_5$-1 NL and (c) $Ge_3Sb_2Te_6$-1 UL under -4% and +4% strains.

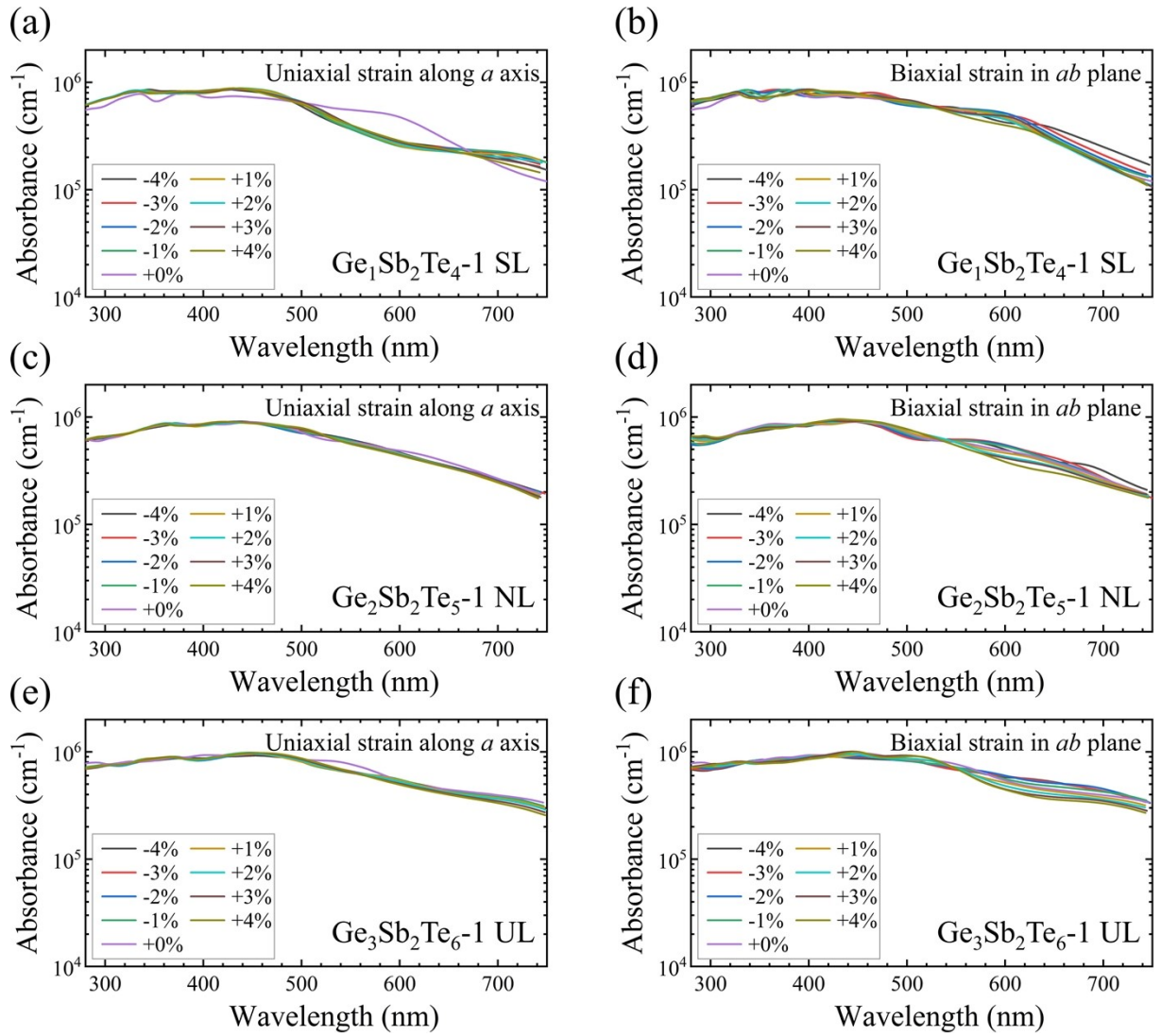

Fig. S13 Optical absorption coefficients of (a, b) $Ge_1Sb_2Te_4$-1 SL, (c, d) $Ge_2Sb_2Te_5$-1 NL and (e, f) $Ge_3Sb_2Te_6$-1 UL under various uniaxial and biaxial strains.

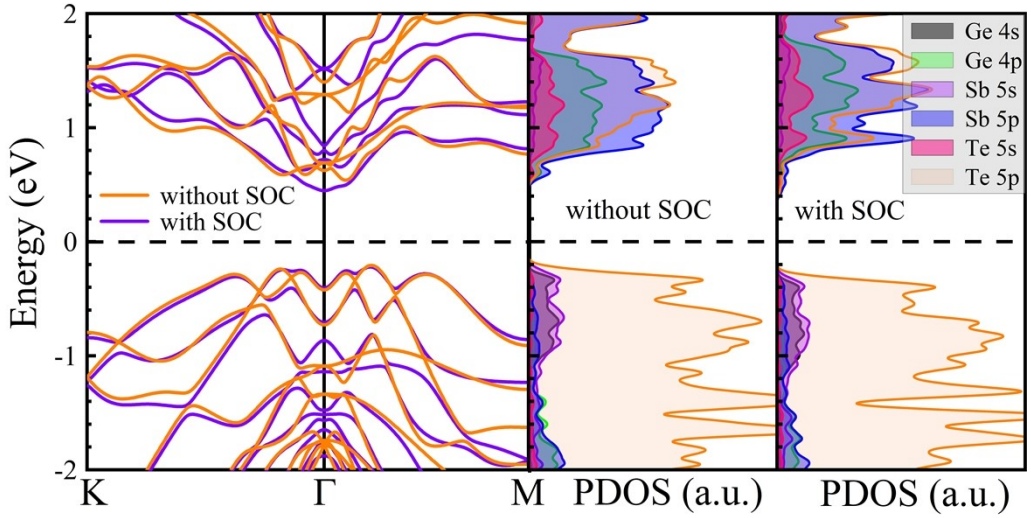

Fig. S14 Calculated electronic band structures and projected density of states with and without spin-orbit coupling (SOC) for $Ge_1Sb_2Te_4$-1 SL.

Taking $Ge_1Sb_2Te_4$-1 SL as an example, we have calculated its electronic structures by including the spin-orbit coupling (SOC) at the PBE level, as shown in Fig. S14. It turns out that the overall shape of electronic bands and projected density of states with SOC are similar to those without SOC. Interestingly, the conduction band minimum (CBM) locating between Γ and M points without SOC, moves to Γ point with SOC, suggesting that SOC has a relatively stronger effect on the conduction band edges than the valence band edges due to the heavier constituent element Te. Nonetheless, the indirect electronic bandgap and the direct-indirect bandgap difference of $Ge_1Sb_2Te_4$-1 SL with SOC are close to the values calculated without SOC, indicating that SOC would have little impact on the optical performance.

References

(1) S. Saha, T. P. Sinha, A. Mookerjee, *Phys. Rev. B*, 2000, **62**, 8828.

(2) R. King-Smith, D. Vanderbilt, *Phys. Rev. B*, 1993, **47**, 1651.

(3) W. Shockley, H. J. Queisser, *J. Appl. Phys.*, 1961, **32**, 510-519.

(4) L. P. Yu, A. Zunger, *Phys. Rev. Lett.*, 2012, **108**, 5.